Investigation of the Initial Steps of the Electrochemical Reduction of CO_2 on Pt Electrodes

Kalyan Dhar and Carlo Cavallotti*

Dept. di Chimica Materiali e Ingegneria chimica "G. Natta", Politecnico di Milano, via Mancinelli 7, 20131 Milano, Italy

1. INTRODUCTION

The catalytic reduction of carbon dioxide is a reaction that lies at the heart of many natural as well as industrial processes, such as the carbon cycle, catalytic combustion of hydrocarbons, and electrochemical conversion of CO_2 to formic acid or carbon monoxide. For this reason the CO_2 reactivity at metal centers has been the subject of many experimental and theoretical investigations. Several reviews covering fundamental as well as applied aspects of this process are available in the literature.[1−5] As the problem of controlling CO_2 emissions has grown considerably in the past decade and promises to be a critical issue also for the years to come, as pointed out in the latest IPCC report, the possibility of exploting existing technologies to convert CO_2 to higher-value products has been receiving increasing attention. In particular, electrochemical processes offer a promising route for making CO_2 react while containing the energetic costs and controlling the selectivity. The electrochemical reduction of CO_2 has been the subject of much study in the last 30 years.[1−3,6,7] It is thus known that the activation of CO_2 at an electrode surface requires reaching a significant electronegative potential, which is often explained in terms of the energetic cost that is required to form the highly reactive $CO_2^{\bullet-}$ radical anion. The standard potential usually reported for the $CO_2/CO_2^{\bullet-}$ couple in DMF in a 0.1 M NEt_4-ClO_4 electrolyte is −2.21 V vs SCE, measured on a Hg electrode.[8] The main products of CO_2 electrochemical reduction are a function of the electrode material and the composition of the electrolyte. The chemical species found most often as reaction products are formic acid, oxalate, and carbon monoxide. A systematic study of the products of CO_2 reduction as a function of the electrode material was performed by Hara et al. by exposing the electrodes to high CO_2 partial pressures of 30 bar.[9]

The proposal that $CO_2^{\bullet-}$ is formed at the electrode surface was advanced by several authors a few decades ago.[10,11] The evidence for the formation of the $CO_2^{\bullet-}$ species was indirect and was in one case[11] related to the observation through Fourier transfrom infrared (FTIR) spectroscopy of a wide absorption band centered around 1680 cm^{-1} on Pt electrodes exposed to CO_2 dissolved in acetonitrile (ACN) at high cathodic potentials. It was thus proposed that the high overpotential needed to reduce CO_2 was necessary to distort it from its linear structure to form a radical CO_2 anion having a trigonal planar structure, which is known to be characterized by an asymmetric stretching frequency of about 1700 cm^{-1}. On this basis, several mechanisms of CO_2 reduction have been proposed. The ample literature of this important subject has been reviewed recently by Chaplin and Wragg,[1] who summarized the different reaction mechanisms that have been proposed to describe the electrochemical CO_2 reactivity.

Despite the relevant amount of work devoted to the study of the mechanism of CO_2 electrochemical reduction, there is not

Received: May 30, 2014
Revised: September 3, 2014
Published: September 4, 2014

yet agreement on which are the main reaction routes for this system. To cite a recent example, while Cuesta et al.[12,13] proposed a few years ago that adsorbed formate is the key intermediate in the oxidation of formic acid (that is the reverse reaction of CO_2 reduction), almost contemporarily Wang and Liu[14] advanced the hypothesis that adsorbed formate is not an intermediate but that it plays a catalytic role in the direct decomposition of adsorbed formic acid. Similarly, the necessity of invoking the formation of such an unstable species as the $CO_2^{\bullet-}$ radical anion has been disputed by several authors,[6] who proposed alternative reaction mechanisms that involved an adsorbed CO_2 reaction intermediate. The field of study of the mechanism of CO_2 electrochemical reduction has recently been further enriched by the quite interesting finding that it is possible to reduce the overpotential associated with this process if the reaction is performed in the EMIM-BF_4 ionic liquid, thus showing the prominent impact that the environment can have on the reactivity of this system.

The purpose of the present study is to investigate through quantum chemistry the initial stages of the electrochemical reduction of CO_2 on Pt electrodes. The rationale behind the choice of Pt as a reference material for this study is that a significant body of experimental data can be found in the literature for this system and the considerable interest in the use of Pt as an electrode for CO_2 reduction. Simulations were performed both in water and in acetonitrile because these are the two solvents for which most data exists. The investigation of an electrochemical process using a theoretical quantum chemical model is a complex task, as its reactivity is influenced significantly by the environment, the nature and surface structure of the metal electrode, the surfactants introduced in the solvent, and the applied potential. Each one of these aspects poses a challenge to the development of a predictive quantum chemistry model, and this is the reason why only a few quantum chemistry models have been reported in the literature for electrochemical processes involving CO_2 as a reactant. In particular, we cite here the works of Wang and Liu[14] and of Ishikawa et al.,[15] which were devoted to the study of the electrochemical reactivity of formic acid and hydrogen on Pt surfaces, and the work of Shi et al., who studied CO_2 reduction on the Pt(111) surface.[16] In the present study it has been decided to model the effect of solvation using an implicit model while the surface has been modeled using two clusters containing 13 and 20 Pt atoms. The effect of the applied potential has been modeled studying clusters having different total charges. The effect of surfactants that may be present in solution has been neglected at the present stage, which has been mostly focused on the investigation of thermodynamic and structural aspects. In particular, the three points that this work addresses are the following: How does CO_2 adsorbs on Pt electrodes during its electrochemical reduction? How does the nature of the solvent influence the adsorption process? What are the most likely reaction paths for adsorbed CO_2?

2. METHOD

The adsorption of CO_2 on Pt was studied using density functional theory (DFT) and Gaussian basis sets. In particular, the calculations were performed using the Becke three-parameter exchange functional[17] and the Lee, Yang, and Parr correlation functional[18] (B3LYP). The B3LYP hybrid functional has been widely used in the literature to study the hydrocarbon reactivity; therefore, it has been extensively benchmarked.[19−23] It is thus known that it can provide reasonable estimates of reaction energies and kinetic constants, though it can be in error by several kilocalories per mole with respect to experimental data, especially when van der Waals interactions are significant. A new generation of functionals that address the problem of predicting dispersion interactions has been developed in the last years. To test how relevant such effects may be for the system under consideration we compared the interaction energy of the CO_2−Pt complex in water calculated using the B3LYP functional with that determined using the M062X functional,[24] which is able to predict interaction energies in better agreement with experimental data than the B3LYP functional. The calculated interaction energies differ by 1.5 kcal/mol, which can be considered as a reasonable disagreement as it is within the few kilocalories per mole of uncertainties that can be expected from calculations performed at the DFT level. Regarding the use of DFT to study transition metals, both in the gas phase and in solution, we refer to a review recently published by Cramer and Truhlar.[41]

Simulations were performed using three different basis sets, all exploiting effective core potentials. The smallest basis set used in the simulations is composed by the effective core potentials (ECP) developed by Hay and Wadt for Pt,[25−27] thus inclusive of relativistic corrections (LANL2DZ), and the double-ζ basis set of Dunning[28] for C, H, and O atoms (D95). The second basis set used in the simulations is composed by the small core Stuttgart Dresden basis set for Pt[29,30] and the 6-311+G(d,p) basis set for C, H, and O atoms, while the third uses the CRENBL basis set developed by Ross et al.[31] for Pt and the 6-311+G(d,p) basis set for the light atoms. Though all ECPs substitute 60 core electrons with potentials, the Stuttgart Dresden and CRENBL basis sets use a triple-ζ basis set to describe the valence electrons, while the LANL2DZ basis set uses a double-ζ basis set. The motivation for the choice of these basis sets to perform the simulations as well as a benchmark against experimental data is given in section 3.1 All simulations were performed using 6 D and 10 F Cartesian functions. The use of a triple-ζ basis set for the first row elements was preferred over that of a smaller basis set for the SDD and CRENBL basis sets as it allows calculating more accurate vibrational frequencies. To quantify the expected error, the C═O and C−O stretching frequencies computed at the B3LYP/6-311+G(d,p) level for acetic acid (CH_3COOH) in the gas phase are 1817 and 1205 cm^{-1}, thus only slightly overestimating the experimental values[32] by 29 and 23 cm^{-1}, respectively.

The structural optimization of all the structures located in the present study was followed by a frequency analysis. Minimum energy structures are characterized by the absence of negative vibrational frequencies, while transition states have a single imaginary frequency.

The electrode surface was modeled using two clusters of different size, the first containing 13 and the second 20 Pt atoms. A large body of literature focused on the study of structures of Pt clusters is available;[33−37] therefore, there was no need to perform a conformational search to determine the minimum energy structures. The two surface models differ not only for the number of atoms considered but also for the applied constraints. In the first case, the structure of the cluster used in the simulations is the minimum energy structure of the 13 Pt atoms. It was determined using as a starting guess the structure determined by Chou et al.,[37] who performed an extensive conformational study of this system, and was then fully optimized at the three computational levels used in this

work. The second structure used in the simulations is the 20-atom Pt cluster adopted by Daramola and Botte[36] to study the adsorption of ammonia on Pt surfaces. This model was developed to mimic the Pt(111) surface. Several of the atoms composing the cluster are for this purpose constrained to their lattice positions, while only the core atoms are allowed to relax. Structures for Pt20 clusters solvated in water were optimized at the B3LYP/LANL2DZ level, while energies were computed using the three basis sets. Some test simulations performed fully optimizing the geometries of Pt20 complexes in water showed that this approximation is quite reasonable for what concerns the estimation of adsorption free energies. For simulations performed in acetonitrile, structures were optimized at the same level used to determine the energies. For all the calculations here performed that involve Pt clusters, different spin states were considered, and interaction energies were always computed for the ground state. In a few cases, interaction energies calculated for spin states that differ slightly from that of the ground state are also reported. To test the effect that the application of a high cathodic potential may have on the CO_2 binding process, the binding energy between solutes and clusters was computed changing the total charge of the cluster. It is in fact reasonable to assume that the application of a cathodic potential to the electrode will lead to the formation of a negatively charged Pt layer at the liquid−solid interface.

All simulations were performed modeling the solvent implicitly using the polarizable continuum model (PCM),[38,39] thus computing the electrostatic free energy of interaction (ΔG_{pol}) of a solute immersed in a polarizable continuum. To support the choice of the adopted computational protocol, it should be noted that implicit solvation models have been amply used to study Pt complexes in solution.[22,23,40] An assessment of the use of the PCM model in conjunction with the B3LYP functional and the 6-311+G(d,p) basis set to determine vibrational frequencies of solvated molecules has been recently published by Cappelli et al.[42] The SMD model[43] was used to determine the cavitation (ΔG_{cav}) and nonelectrostatic (dispersion) (ΔG_{dis}) contributions, which were added to the electrostatic energy of the solute. Interaction free energies were computed as the difference between the free energy of the complex and that of the reactants. The energies so determined are thus equal to gas-phase energy differences corrected for solvation energies. As such, a gas-phase entropic correction should be added to complete the Born−Haber cycle and evaluate the reaction free-energy change. The entropic correction is reported separately in Results and Discussion, as it is our opinion that the accurate calculation of entropic corrections should be performed considering explicitly the effect of the solvent, in particular for what concerns the vibrational contribution. The reported values should thus be considered as a first level approximation of the real entropic contributions. The interaction free energy between CO_2 (or CO, CO_2H, and HCO_2) and the clusters was thus determined as

$$\Delta G_{int} = \Delta E_{el} + \Delta\Delta G_{pol} + \Delta\Delta G_{cav} + \Delta\Delta G_{dis} + \Delta ZPE \quad (1)$$

To describe more properly the perturbation of the solvent adlayer on the Pt surface that is determined by the adsorption of the reactant, interaction energies were also computed in a few cases as the free energies required to substitute one adsorbed water molecule with the adsorbate. For the adsorption of CO_2, the global reaction considered was

$$CO_2 + H_2O_{ads} \rightarrow CO_{2ads} + H_2O \quad (R1)$$

The interaction free energies were in this case computed as in eq 1.

The zero-point energy (ZPE) used to correct the energies determined for the Pt20 cluster were computed at the B3LYP/LANL2DZ level, while the ZPE used for the Pt13 clusters were always computed at the same level of theory used to optimize the structures.

For the calculation of the protonation free energy of adsorbed CO_2, two explicit water molecules were added to the model, as it is known that for the calculation of pK_a values the explicit consideration of several solvent molecules is needed to obtain reliable results.[44] The approach used to determine the protonation free energy is similar to the one used for the estimation of accurate thermochemical parameters through isodesmic reactions,[45,46] as the reaction free-energy change is computed as the change of free energy with respect to a reference reaction.

Charge transfers from clusters to CO_2 adatoms were determined from natural bond orbital (NBO)[47] populations and electrostatic charges.[48] In the last case, a crystallographic van der Waals radius of 2.06 Å was used in the calculations.[49]

All calculations were performed with the Gaussian 09 suite of programs.[50] Molecular structures were drawn with Molden.[51]

3. RESULTS AND DISCUSSION

The results of the simulations are presented in five sections: The first reports a benchmark of the adopted computational approach. The second is focused on the study of the structural and energetic aspects related to CO_2 adsorption on Pt in acetonitrile and water solvents. The third is focused on CO_2 adsorption kinetics. The fourth investigates the reaction of formation of the HCO_2 intermediate. The fifth explores the possible reaction routes of adsorbed CO_2.

3.1. Benchmark of Computational Approach. The adopted computational methodology was benchmarked calculating the binding energies for the Pt dimer and for the gas-phase adsorption of CO on the Pt surface, for which experimental data are available, as well as calculating the adsorption free energy of CO_2 on the Pt surface in water, whose interaction with the surface plays a central role in the present study and requires therefore a careful evaluation of the impact of the choice of the basis set on the simulation results. For this purpose the interaction energies were computed using several basis sets and the Pt13 cluster, wiht the exception of two simulations performed with the Pt20 cluster with the aim of determining the convergence with the cluster size. The basis sets for Pt considered in the benchmark are the three basis sets used in the present study (LANL2DZ, SDD, and CRENBL), the triple-ζ basis set DEF2TZVPP of Weigend and Ahlrichs,[52] which uses Stuttgart-Dresden ECP for 60 core electrons,[29] the triple-ζ basis set DHFTZVPP of Weigend and Baldes,[53] which uses as well Stuttgart-Dresden ECP for 60 core electrons, and the LANLTZ basis set,[54] which uses a triple-ζ basis set for valence electrons and the Hay and Wadt basis set for 60 core electrons.[26] The basis sets used for C and O are the 6-311+G(d,p) basis set used in the present study and the aug-cc-pVTZ basis set.[55] The basis sets used in the simulation were downloaded from the Environmental Molecular Sciences Laboratory Web site,[56,57] with the exception of the LANL2DZ

and SDD basis sets, which were used as implemented in Gaussian 09. The results of the calculations are reported in Table 1.

Table 1. Gas-Phase Binding Energies of the Pt_2 Dimer, Gas-Phase Adsorption Energies (kcal/mol) of CO on Pt13 Clusters, and Adsorption Free Energies of CO_2 on Pt13 Clusters (Not Corrected for the Entropy Change) Calculated at Different Levels of Theory[a]

Pt basis set	C, O basis set	ΔE Pt−Pt (kcal/mol)	ΔE CO−Ptn (kcal/mol)	ΔG_{wat} CO_2−Ptn[b] (kcal/mol)
LANL2DZ	D95	52.2	35.1	−20.5
LANL2DZ	6-311+G(d,p)	52.2	51.0	−34.9
SDD	6-311+G(d,p)	58.1	29.4	−9.3
CRENBL	6-311+G(d,p)	53.0	36.0	−12.2
DEF2TZVPP	6-311+G(d,p)	64.6	40.6	−11.1
DHFTZVPP	6-311+G(d,p)	65.4	36.8	−14.5
LANLTZ	6-311+G(d,p)	70.6	31.3	−19.0
SDD	aug-cc-pVTZ	58.1	31.8	−8.7
LANL2DZ	D95	52.2	32.7[c]	−18.8[c]
SDD	6-311+G(d,p)	58.1	26.1[c]	−5.1[c]
experimental		73.8 ± 0.5[d]	32.3 ± 3[e]	–

[a]Adsorption free energies on Pt20 clusters are reported for comparison at the bottom of the table. [b]The entropic correction is +10.3 kcal/mol calculated at the B3LYP/SDD-6-311+G(d,p). [c]Calculated using the Pt20 cluster. [d]Airola and Morse.[58] [e]Abild-Pedersen and Andersson.[59]

The results reported in Table 1 show that all basis sets underestimate the binding energy of the Pt dimer and that the best agreement is obtained using the LANLTZ basis set. Increasing systematically the basis set improves considerably the agreement between calculated and experimental data, as a relatively good agreement is found for the DHFTZVPP basis set, which is the largest considered in this study. Despite the significant dependence on the basis set found in the prediction of the Pt binding energies, the gas-phase adsorption energies of CO on the Pt surface are in a relatively good agreement among them and with the experimental value, with the exception of the DEF2TZVPP and the LANL2DZ-6-311+G(d,p) basis sets, which were therefore not further considered in the present study. The vibrational frequency for CO adsorbed on the Pt13 cluster in the top configuration calculated at the B3LYP/SDD-6-311+G(d,p) level is 2095 cm^{-1}, which is in good agreement with the literature values measured for CO on Pt(111) surfaces that are between 2083 and 2100 cm^{-1}[60] and the 2020 cm^{-1} value determined by Gruene et al. for Pt clusters containing between 3 and 25 metal atoms.[61] The clusters used in the present analysis are unable to discriminate for adsorption between the hollow and the top sites on a Pt(111) surface, a subject on which there has been considerable discussion in the literature.[62] However, it is noteworthy that the gap between the highest occupied molecular orbital and the lowest unoccupied molecular orbital calculated at the B3LYP/6-311+G(d,p) level is 9.2 eV, which is in good agreement with the gap calculated using the PBE0 exchange functional (9.42 eV) that was found by Wang et al.[63] to be a key parameter to adequately describe the interaction of CO with the Pt(111) surface.

The analysis of the interaction energy between CO_2 and the Pt13 cluster in water shows that it depends significantly on the ECPs used in the calculations, with the LANL potentials predicting interaction free energies significantly higher (in absolute value) than those calculated using the CRENBL and the Stuttgart-Dresden ECPs. Because no experimental data is available for what concerns the CO_2 adsorption free energy on Pt in water, the simulations were performed using three basis sets that are representative of the three different ECPs considered in this study: LANL2DZ, CRENBL, and SDD. The LANL2DZ-D95 basis set was preferred over the LANLTZ-6-311+G(d,p) basis set as both predict similar CO and CO_2 interaction energies and the LANL2DZ-D95 basis set is considerably smaller. The 6-311+G(d,p) basis set was used for the light atoms for all the calculations, though the simulation performed using the aug-cc-pVTZ basis on the light atoms shows that the use of large basis may affect the computational results by about 2 kcal/mol. The analysis of the interaction energies of CO and CO_2 for Pt13 and Pt20 clusters shows that the interaction energies calculated with Pt20 clusters are systematically smaller than those determined for the Pt13 clusters by 3−4 kcal/mol. As is shown in the following sections, this is a difference that is observed also for CO adsorption in solution and for the adsorption of COOH and HCO_2 on the Pt surface. This difference can be due either to a systematic decrease of the interaction energy with the increase of the cluster size, as for example found for CO adsorption on Pd,[64] or to a different reactivity of the two clusters, determined by the fact that the Pt13 cluster is a minimum energy structure and the Pt20 cluster is a portion of the Pt(111) surface with part of the geometry frozen in place through apposite constraints. The result is that the Pt20 cluster has a ground-state electronic structure with a high spin multiplicity, which may interfere with the reactivity of the most coordinated Pt atoms. This aspect will be further discussed in the next section.

3.2. CO_2 Adsorption. The adsorption of CO_2 was studied considering two different clusters to model the Pt surface, two different solvents, water and acetonitrile, and three different electronic states, which differ for the imposed total charge: neutral, −1, and −2. The minimum energy structures of the neutral clusters calculated at the B3LYP/SDD-6-311+g(d,p) level in water are shown in Figure 1. CO_2 was adsorbed on the top layer of the two clusters, which is the most dense of the three atomic layers that compose the clusters. In particular, the Pt13 cluster has 8 atoms in the first layer, 4 in the second and 1 in the third, while the Pt20 cluster has 10, 5, and 5 Pt atoms in the first, second, and third layers, respectively. The cohesive energies calculated in water are −63.8 and −64 kcal/mol for the LANL2DZ and SDD-6-311+g(d,p) basis sets for the Pt13

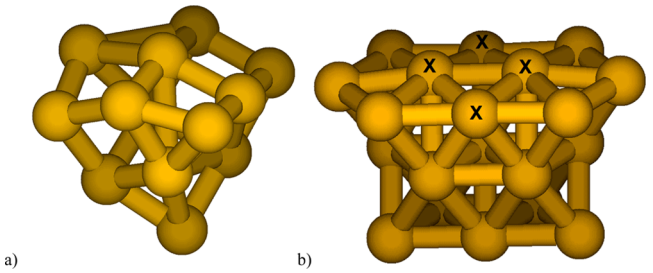

Figure 1. Structure of the Pt 13 (a) and Pt20 (b) clusters used in the simulations. The Pt 13 cluster was fully optimized, while only the four central atoms of the top layer (each marked with X) of the Pt20 cluster were allowed to relax. It should be noted that the two central atoms at the edge of the cluster are coordinatively unsaturated. All the other atoms were held fixed in the FCC lattice positions of the Pt crystal.

cluster and −64.2 and −64.1 kcal/mol for the Pt20 cluster, which is in good agreement with the −65.2 kcal/mol cohesive energy in the gas phase calculated by Daramola and Botte for the Pt20 cluster at the B3LYP/LANL2DZ level.[36] This shows that the cohesive energy, and thus the electronic structure of the cluster, is only slightly affected by solvation. The spin multiplicity of the Pt13 and Pt20 neutral clusters are 3 and 15 and decrease to 2 and 1 and to 14 and 13 when the clusters are singly and doubly negatively charged, respectively. Spin multiplicities are also not significantly affected by solvation.

An extensive conformational study showed that CO_2 can adsorb on Pt clusters in two configurations: top and bridge. In the top structure, a single bond is formed between the CO_2 carbon atom and a Pt atom, while in the bridge structure a second bond, involving the oxygen atom and a neighboring Pt atom is present. In general, the top structure is more stable than the bridge structure, in particular when the cluster is charged. Also, in several cases it was not possible to optimize the bridge structure as the geometry systematically converged to the top structure, indicating that the energetic barrier between the two structures is minimal. Bidentate structures in which CO_2 is bound to Pt through two bonds involving the two oxygen atoms could also be optimized in a few cases, though the interaction energy is considerably smaller than that of the top and bridge structures. The minimum energy top and bridge structures calculated for the adsorption of CO_2 on the neutral Pt13 cluster in water are shown in Figure 2. CO_2 adsorption

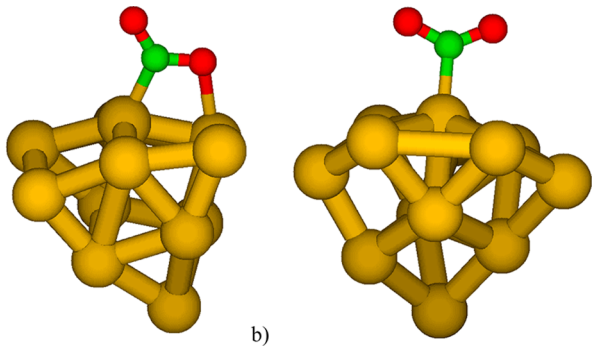

Figure 2. Minimum energy structures of CO_2 adsorbed on a Pt13 neutral cluster calculated at the B3LYP/SDD-6-311+G(d,p) level: bridge (a) and top (b).

energies calculated using eq 1 are reported in Table 2 for the water solvent and in Table 3 for acetonitrile, together with the ground-state spin multiplicities. The results of simulations performed with spin multiplicities different from that of the ground state are reported in a few cases when the adsorption energies do not differ substantially from those calculated with the ground-state multiplicity.

The results reported in Tables 2 and 3 show that, as found in section 3.1, the calculated adsorption energies are significantly influenced by the basis set adopted for the calculations, with LANL2DZ and SDD-6-311+G(d,p) or CRENBL-6-311+G-(d,p) results differing by about 10 kcal/mol. Despite this, the interaction energy trends are in general in qualitative agreement, though in some cases the calculations performed with the LAN2DZ basis set mispredict the most stable structure and the ground-state multiplicity with respect to what was found using the other basis set, and in one case (adsorption on water, charge −2) a significant deviation from the expected trend is observed. In the latter case, an additional simulation performed at the LANLTZ level gave a result in agreement with those calculated with the other basis sets, thus indicating that in some cases the results obtained with the LANL2DZ basis set should be carefully considered.

Adsorption energies calculated for uncharged clusters using the SDD-6311+G(d,p) basis sets predict a CO_2 adsorption free energy of about 1−3 kcal/mol, with the exception of adsorption in water over the Pt13 cluster, in which case a significant interaction free energy of about 10 kcal/mol is determined. The interaction free energies computed with the CRENBL-6-311+G(d,p) basis sets follow the same trend but predict an interaction free energy that is about 3 kcal/mol higher. It can also be observed that the interaction free energies calculated using the Pt13 cluster are in general slightly higher than those determined using the Pt20 cluster for uncharged clusters, as anticipated in section 3.1, while a significant difference is found for charged clusters, which was further investigated performing a population analysis as described in the following.

The calculated high adsorption energy for CO_2 on Pt13 in water is consistent with the high adsorption rate observed for CO_2 on Pt surfaces in water,[4] which is known to lead rapidly to the decomposition of CO_2 and to the formation of a poisoning CO layer. Also, the difference of adsorption free energies computed between water and acetonitrile is consistent with the decrease of reactivity observed between the two solvents.[65] When the clusters are negatively charged, the interaction free energies increase significantly in water and in acetonitrile on the Pt13 cluster, while this effect, though present, is less evident on Pt20 clusters. This is consistent with the observation that the reactivity of CO_2 on Pt is enhanced with the increase of the cathodic potential, in particular when the solvent is acetonitrile.[65] Indeed, the present simulations indicate that the adsorption of CO_2 on Pt surfaces becomes favored in acetonitrile only when the surface is negatively charged.

As the simulations reveal that the effect of the solvent is significant in favoring the adsorption of CO_2 on the Pt surface, it is interesting to investigate in more detail what determines the formation of the chemical bond between CO_2 and Pt and how the adsorption process modifies the CO_2 structure. For this reason, some selected geometric and electronic structure parameters are reported in Table 4 for the ground-state electronic structures of the complexes whose adsorption energies are reported in Tables 2 and 3.

The analysis of the structural parameters reported in Table 4 shows that the adsorption process modifies significantly the structure of CO_2, with the O−C−O angle changing from 180° to about 125−135°. This can be interpreted in terms of an sp2 hybridization of the s and p valence orbitals of the carbon atom. The relatively small C−Pt distance, ranging between 2.03 and 2.14 Å, is also indicative of the formation of a chemical bond. The calculated charge transfer indicates that the nature of this bond is dative, with the charge transferred from the Pt cluster to CO_2. The NBO analysis shows that the Pt atom involved in the Pt−C bond has the p valence orbitals partially filled, which suggests that the formation of the Pt−C bond requires to some extent the promotion of electrons from the Pt cluster to the 6p orbitals of the Pt atom involved in the bond. The amount of charge transfer depends on the solvent, with the largest charge transfers found in the most polar solvent, which is water, as it could be reasonably expected. Also, it is interesting to observe that the charge transfer is only slightly dependent on the total charge of the cluster. In particular, it can be observed that the transfer of charge to CO_2 in the neutral cluster in water with

Table 2. Adsorption Free Energies (kcal/mol) of CO_2 on Pt13 and Pt20 Clusters calculated at the B3LYP/LANL2DZ, B3LYP/SDD-6-311+G(d,p), and B3LYP/CRENBL-6-311+G(d,p) Levels in Water[a]

conformation	cluster	charge	multiplicity	ΔG LANL2DZ D95	ΔG SDD 6-311+g(d,p)	ΔG CRENBL 6-311+g(d,p)
top	Pt13	0	3	−20.5	−9.3 (−7.3)	−12.2 (−9.0)
bridge	Pt13	0	3	−16.1	−1.9 (+0.1)	−7.1 (−4.0)
top	Pt20	0	15	–	−8.1[b]	−9.6[b]
bridge	Pt20	0	15	−18.8	−5.1	−6.4
top	Pt13	−1	2	−27.3	−15.6 (−12.9)	−18.0 (−14.1)
top	Pt13	−1	4	−26.2	−14.5	−16.3
top	Pt20	−1	14	−22.8	−9.4	−9.3
bridge	Pt20	−1	14	−20.2	−5.2	−5.8
top	Pt13	−2	13	−59.6[c]	−20.3 (−15.7)	−22.4 (−16.8)
top	Pt20	−2	13	−24.1	−10.3	−11.1
bridge	Pt20	−2	13	−21.9	−6.5	−8.2

[a]All energies corrected for ZPE calculated at the same level of theory for Pt13 clusters and using the LANL2DZ basis set for Pt20 clusters. If no energy is reported, it means that the calculation did not converge to the desired structure, but to the other conformer. The adsorption free energies reported between parentheses were computed using reaction R1, thus accounting for the displacement of one water molecule adsorbed in the first solvation shell on the Pt surface. The entropic correction, not included in the reported free energies, is about +10 kcal/mol (at the B3LYP/SDD-6-311+G(d,p) level on Pt13; it is +3.2 kcal/mol when a water molecule displacement is explicitly considered in the calculations), and it is essentially independent of cluster size, basis set, and total charge. [b]Structure optimized at the same level of theory used to calculate the energy. [c]The adsorption energy is −24.1 kcal/mol when calculated using the LANLTZ-6-311+G(d,p) basis set.

Table 3. Adsorption Free Energies (kcal/mol) of CO_2 on Pt13 and Pt20 Clusters Calculated at the B3LYP/LANL2DZ, B3LYP/SDD-6-311+G(d,p), and B3LYP/CRENBL-6-311+G(d,p) Levels in Acetonitrile[a]

conformation	cluster	charge	multiplicity	ΔG LANL2DZ D95	ΔG SDD 6-311+g(d,p)	ΔG CRENBL 6-311+g(d,p)
top	Pt13	0	3	−11.0[b]	−1.8	−4.1
bridge	Pt13	0	3	−11.9	−1.8	−5.1
top	Pt20	0	15	–	−0.8	−1.6
bridge	Pt20	0	15	−16.2	−1.3	−2.9
top	Pt13	−1	2	−14.9	−7.4	−10.0
top	Pt13	−1	4	−17.5	−6.4	−7.3
bridge	Pt13	−1	2	−20.9	−7.4	−9.2
top	Pt20	−1	14	–	−4.4	−3.2
bridge	Pt20	−1	14	−15.8	−2.0	−2.7
top	Pt13	−2	1	−26.6	−11.8	−13.2
bridge	Pt13	−2	1	−25.9	–	–
top	Pt20	−2	13	−15.2	−3.8	−4.1
bridge	Pt20	−2	13	−17.6	−2.2	−3.3

[a]All energies corrected for ZPE calculated at the same level of theory for Pt13 clusters and using the LANL2DZ basis set for Pt20 clusters. If no energy is reported, it means that the calculation did not converge to the desired structure, but to the other conformer. The entropic correction, not included in the reported free energies, is about +9 kcal/mol (at the B3LYP/SDD-6-311+G(d,p) level on Pt13), and it is essentially independent of cluster size, basis set, and total charge. [b]Energy and structure optimized with a spin multiplicity of 5, as the calculations performed with a spin multiplicity of 3 converge to the bridge structure.

CO_2 adsorbed in the top conformation (−0.73) is only slightly different from that determined for the doubly charged cluster in the same conformation (−0.80). This was in part unexpected, as the difference in interaction energy between CO_2 adsorbed on the two clusters is large, as it increases by about 10 kcal/mol going from the uncharged to the doubly charged cluster. The analysis of the decomposition of the free interaction energy according to eq 1 shows that the increase in interaction energy is not determined by dispersion or cavitation effects, so that it can mostly be ascribed to a change of the polarization free energy. The following interpretation may explain this evidence. When CO_2 gets adsorbed on a cluster, a partial charge is transferred from the cluster to CO_2. If the cluster is neutral this means the cluster gets positively charged, which leads in turn to a decrease of the interaction energy of the cluster with the solvent, in particular if the solvent is polar. As the cluster becomes negatively charged, this polarization effect becomes less evident. Indeed it can be noted that the free interaction energy between CO_2 and Pt increases most significantly when the system becomes singly negatively charged (+5.7 kcal/mol in water, + 5.6 kcal/mol in acetonitrile, top configuration) than when the charge increases from −1 to −2 (+4.7 kcal/mol in water, + 4.5 kcal/mol in acetonitrile, top configuration). This is particularly evident if the free-energy change is computed accounting for the energy required to displace an adsorbed water molecule using the data reported between parentheses in Table 2. In this case the free adsorption energy of CO_2 increases by +5.7 kcal/mol as the cluster charge changes from 0 to −1, and it increases only by +2.8 kcal/mol when it goes from −1 to −2.

The data reported in Table 4 allow us to further investigate what determines the difference in interaction energies computed using the Pt13 and Pt20 charged clusters. The charge-transfer analysis shows that different predictions of the two clusters can be related to the different transfer of charge from the Pt13 and Pt20 clusters to CO_2. The differential

Table 4. Geometric Parameters (O−C−O Angle in Degrees and C−Pt Distance in Angstroms), Charge Transfer to CO_2, and O−C−O Asymmetric Stretch Frequency Calculated at the B3LYP/SDD-6-311+g(d,p) Level for the Ground States of the Pt13 and Pt20 Clusters

Water							
conformation	cluster	charge	O−C−O angle	C−Pt distance (Å)	charge transfer (NBO)	charge transfer (ESP)	O−C−O asymmetric stretch (cm^{-1})
top	Pt13	0	129.5	2.05	−0.73	−0.63	1527
bridge	Pt13	0	124.5	2.03	−0.69	−0.60	1524
top	Pt20	0	131.3	2.06	−0.62	−0.59	–
bridge[a]	Pt20	0	131.2	2.06	−0.52	−0.28	–
top	Pt13	−1	129.0	2.04	−0.75	−0.64	1512
top[a]	Pt20	−1	136.7	2.13	−0.52	−0.52	–
bridge[a]	Pt20	−1	131.1	2.06	−0.56	−0.37	–
top	Pt13	−2	127.7	2.03	−0.80	−0.76	1483
top[a]	Pt20	−2	135.9	2.13	−0.56	−0.56	–
bridge[a]	Pt20	−2	130.1	2.05	−0.59	−0.39	–
Acetonitrile							
conformation	cluster	charge	O−C−O angle	C−Pt distance (Å)	charge transfer (NBO)	charge transfer (ESP)	O−C−O asymmetric stretch (cm^{-1})
top	Pt13	0	135.2	2.10	−0.55	−0.47	1722
bridge	Pt13	0	131.7	2.06	−0.57	−0.41	1660
top	Pt20	0	138.0	2.16	−0.41	−0.41	–
bridge	Pt20	0	131.2	2.06	−0.22	−0.20	1673
top	Pt13	−1	134.9	2.10	−0.54	−0.47	1716
bridge	Pt13	−1	131.7	2.06	−0.59	−0.48	1648
top	Pt20	−1	136.7	2.14	−0.43	−0.44	–
bridge	Pt20	−1	131.1	2.06	−0.45	−0.19	–
top	Pt13	−2	133.5	2.08	−0.59	−0.56	1682
top	Pt20	−2	135.9	2.13	−0.49	−0.55	–
bridge	Pt20	−2	130.1	2.05	−0.47	−0.27	1645

[a]Structures optimized at the B3LYP/LANL2DZ level.

analysis of the electron population of the doubly charged and uncharged clusters shows that in the Pt20 cluster most of the charge (−1.8) is localized on the less coordinated Pt atoms (on the 8 external atoms of the top layer (−1.1), and on the 5 atoms of the bottom layer (−0.7)). As the spin multiplicity of the Pt20 cluster is quite high (15), it is thus likely that in the larger cluster most of the additional charge will be localized on the less coordinated Pt atoms, thus leading to a fictitious underestimation of the interaction energy between the cluster and CO_2. This suggests that the Pt13 cluster may describe the bonding between CO_2 and the Pt surface more properly than the Pt20 cluster when the cluster is charged.

Finally, it is important to observe that the vibrational frequency data reported in Table 4 predict that the asymmetric vibrational frequency of adsorbed CO_2 in acetonitrile should be range between 1640 and 1720 cm^{-1}, a value that is in very good agreement with the 1680 cm^{-1} band measured by Chandrasekaran and Bockris[11] using FTIR spectroscopy when CO_2 was dissolved in acetonitrile in the presence of a Pt electrode kept at high cathodic potentials.

3.3. CO_2 Adsorption Kinetics. The kinetics of the CO_2 adsorption process was investigated by scanning the potential energy surface of the adsorption reaction as a function of the C−Pt bond distance using the Pt13 cluster model. It was thus found that for both neutral and charged clusters, in acetonitrile and water, the reaction proceeds passing from a transition state. The transition-state structures calculated at the B3LYP/SDD-6-311+G(d,p) level for the adsorption of CO_2 in water on a neutral and negatively charged (−1) Pt13 cluster are shown in Figure 3, while some key geometric and energetic parameters are summarized in Table 5.

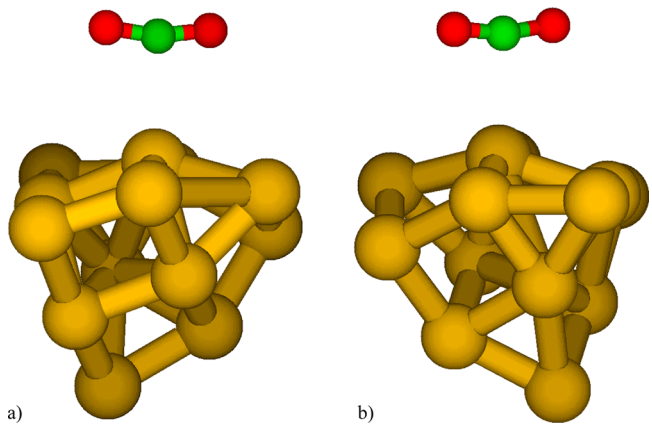

Figure 3. Transition-state structures for the adsorption of CO_2 on a neutral (a) and negatively charged (b) Pt13 cluster calculated at the B3LYP/SDD-6-311+G(d,p) level. The Pt−C distances and O−C−O angles are (a) 2.81 Å and 164.6° and (b) 2.88 Å and 165.8°, respectively.

The data reported in Table 5 show that the adsorption of CO_2 is activated by 2−3 kcal/mol when the system is globally neutral, while a submerged barrier is present when the adsorption takes place in acetonitrile on a negatively charged cluster. The presence of a transition state with a submerged barrier is indicative of the fact that the adsorption of CO_2 involves the formation of a precursor state. The energy of the precursor-state calculated with respect to the reactants is reported as well in Table 5. Interestingly, the adsorption activation energies in water are larger than those in acetonitrile, thus indicating that polarity of the solvent does not contribute

Table 5. Structural Geometric Parameters (O−C−O Angle in Degrees and C−Pt Distance in Angstroms), Activation Free Energies for Adsorption ($\Delta G^{\ddagger}_{ads}$), Charge Transfer to CO_2, and O−C−O Asymmetric Stretch Frequency Calculated at the B3LYP/SDD-6-311+g(d,p) Level for the Transition States of the Reactions of Adsorption of CO_2 on Pt13 Clusters[a]

cluster	charge	O−C−O angle	C−Pt distance (Å)	$\Delta G^{\ddagger}_{ads}$ (kcal/mol)	precursor energy (kcal/mol)	imaginary frequency (cm^{-1})	charge transfer (NBO)
				Water			
Pt13	0	164.6	2.81	4.6	–	−146	−0.01
Pt13	−1	165.8	2.88	1.0	–	−121	−0.01
				Acetonitrile			
Pt13	0	161.6	2.72	3.5	–	−154	−0.024
Pt13	−1	162.4	2.77	−0.3	−1.0	−146	−0.021

[a]The entropic correction to the adsorption free energy (not included) is about +9 kcal/mol.

to the stabilization of the transition state. The minor reactivity of the most polar solvent is confirmed by the fact that the degree of charge transfer is significantly smaller. However, the simulations do indeed reveal that at the transition state the charge transfer is small, though not negligible, and that it is not dependent on the total charge of the system. The potential energy surface calculated at the B3LYP/SDD-6-311+G(d,p) level for the reaction of adsorption of CO_2 on a Pt surface in acetonitrile for a total charge of −1 is shown in Figure 4. The

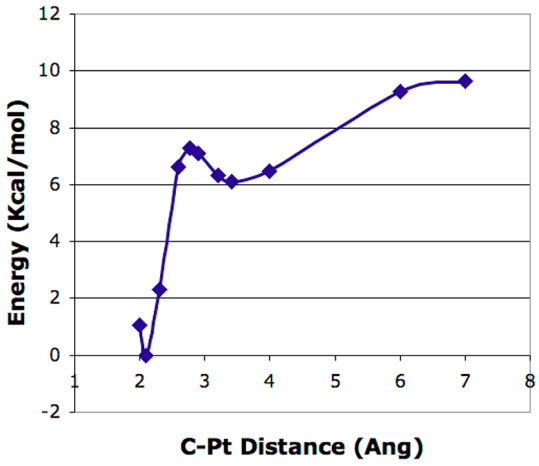

Figure 4. Free-energy surface for the adsorption of CO_2 on a negatively charged Pt13 cluster calculated at the B3LYP/SDD-6-311+G(d,p) level in acetonitrile as a function of the Pt−C distance. Interaction free energies are computed through eq 1 neglecting ZPE contributions.

formation of the precursor state and of the transition state with a submerged barrier can clearly be observed. The calculated charge transfer for this system is 0.02 at the transition state (located at a C−Pt distance of 2.8 Å) and rapidly increases to 0.15 and 0.39 as the C−Pt distance decreases to 2.6 and 2.3 Å, respectively, until a maximum of 0.54 is reached at the equilibrium distance of 2.1 Å.

The thermodynamic analysis of the previous section and the kinetic analysis here performed allow us to draw some preliminary conclusions on the adsorption of CO_2 on a Pt surface in solution. The thermodynamic analysis shows that CO_2 adsorption is energetically favored only if the Pt cluster is negatively charged and that it involves a significant charge transfer to CO_2, which is determined by the establishment of a dative bond between Pt and CO_2. The kinetic analysis shows that the adsorption of CO_2 requires overcoming an energy barrier, after which the CO_2 attractive interaction with the surface leads to the formation of the bond. This evidence suggests that the adsorption of CO_2 on Pt involves a contextual charge-transfer reaction and that the charge will be most probably initially transferred to the Pt atom that will bind CO_2. The structure of the CO_2−Pt system in correspondence to which the charge transfer will take place is most likely located at CO_2−Pt distances between the transition state and the minimum energy structure reached after CO_2 is successfully adsorbed, as the interaction energy becomes significantly attractive in these configurations (see Figure 4). The adsorption reaction may then be described as

$$CO_2 + Pt\_surf + e^- \rightarrow CO_{2ads}{}^-$$

After being formed, $CO_{2ads}{}^-$ may desorb from the surface to give the $CO_2{}^{\bullet -}$ aqueous species whose existence has been proposed in many works focused on the CO_2 reaction kinetics,[10,11] desorb as CO_2, or further react. The free desorption energy for this reaction, calculated on Pt13 clusters using eq 1 in water and acetonitrile for singly and double negatively charged clusters is between 44.4 and 45.5 kcal/mol. It is thus slightly sensitive to the charge of the cluster and to the solvent. As can be observed, these energies are significantly larger than those required to desorb CO_2, which indicates that even if $CO_2{}^{\bullet -}$ is formed through an electron-transfer process, then its main fate would most likely be that of remaining adsorbed on the electrode surface.

An important aspect that is not addressed in the present kinetic calculations is that CO_2 adsorption will lead to the displacement of the first Pt solvent shell. Taking this into account through calculations considering explicitly the solvent molecules is probably necessary in order to study at a greater level of detail the kinetics and energetics of the adsorption process. This is, however, beyond the purpose of the present study.

3.4. CO_2 Protonation: Formation of Adsorbed CO_2H.

The simulations performed in the previous sections show that upon adsorption a significant charge is transferred to CO_2, which will thus behave as a partially charged carboxylic group. As such, it will have an associated acid dissociation constant (pK_a) that will determine its protonation state as a function of pH. The reliability of the computational prediction of pK_a constants has progressed significantly in the last years.[44,45] It has thus been shown that to properly determine reliable pK_a values two approaches are possible: the evaluation of the absolute value by means of simulations considering explicitly a large number of water molecules organized in well-defined structures and exploiting experimental H_3O^+ solvation energies, or the determination of the pK_a as the variation of the free energy of protonation computed relatively to a reference

reaction.[45,46] The latter is the approach here followed. As mentioned in the Method section, the reference compound chosen to calculate the free-energy change associated with the protonation of CO_2 adsorbed over Pt is acetic acid. The $\Delta\Delta G_{Ka}$ is then computed as

$$\Delta\Delta G_{Ka} = \Delta G(CH_3COO^-) - \Delta G(CH_3CO_2H) + \Delta G(Pt\_CO_2H) - \Delta G(Pt\_CO_2^-)$$

The computed free energies include electronic energies; free-energy contributions due to polarization, cavitation, and dispersion; and ZPE corrections. The molecular structures of the anions used in the simulations, shown in Figure 5, include

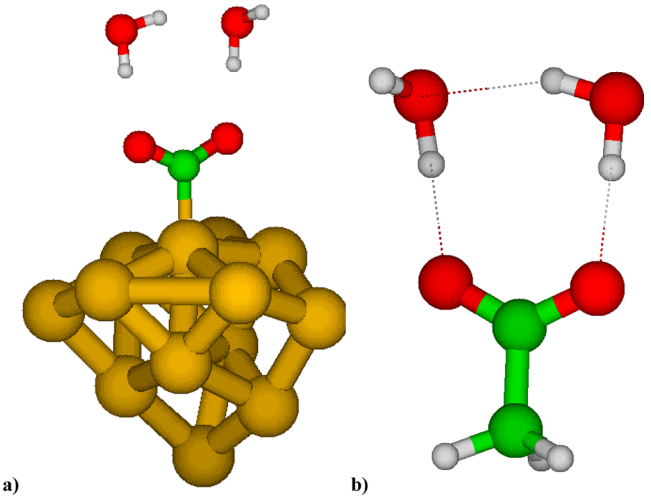

Figure 5. Structures of the anions used to compute relative pK_a values: (a) CO_2 adsorbed over Pt13 in water and (b) acetic acid anion.

two explicit water molecules. The calculated $\Delta\Delta G_{Ka}$, the pK_as, and some relevant geometric parameters are reported in Table 6 for the singly and doubly negatively charged CO_2−Pt13 clusters. The acetic acid pK_a used in the calculations is 4.75.

Table 6. Relative Free Protonation Energy Changes ($\Delta\Delta G_{Ka}$), Absolute Free Energies of Protonation (pK_a), and Some Relevant Geometric Parameters for CO_2 Adsorbed over Singly and Doubly Negatively Charged Pt13 Clusters Calculated at the B3LYP/SDD-6-311+G(d,p) Level in Water

	Pt13_$CO_2(2H_2O)^-$	Pt13_$CO_2(2H_2O)^{-2}$
$\Delta\Delta G_{Ka}$ (kcal/mol)	−2.9	−5.1
ΔG_{Ka} (kcal/mol)	9.4	11.6
pK_a	6.9	8.5
C−Pt distance (Å)	2.03	2.02
O−C−O angle	127.5	126.8

The calculations predict that the pK_a constant of adsorbed CO_2 is about 7−8, which means that at pH values that are neutral or lower than neutral the reaction of protonation of CO_2 will be thermodynamically favored. As the concentration of water is decreased, as is the case when water/acetonitrile mixtures are used, then also the activity of the hydrogen ions will decrease and the reaction of protonation of CO_2 will become increasingly less favored, thus opening alternative reaction pathways that do not involve the formation of CO_2H at the surface as a reaction intermediate. The computational finding that the conversion of CO_2^- to COOH is favored in water is supported by the study of CO_2 reduction over Pt(111) made by Shi et al.,[16] who performed DFT calculations on periodic slabs using the RPBE exchange correlation functional. Their investigation of the reactivity of adsorbed CO_2 confirmed that the proton transfer from water to adsorbed CO_2 is energetically favored and that the energy barrier is relatively small (about 2 kcal/mol).

3.5. Reactivity of Adsorbed HCO_2: Formation of CO and CHO_2. After the reaction of protonation of adsorbed CO_2 is studied, it is interesting to investigate what may be the successive reaction route. For this purpose the analysis was focused on the determination of the structure and adsorption energies of the two most important reaction intermediates that can be formed from CO_2H: adsorbed CO and adsorbed formate (HCO_2). This study is facilitated by the fact that the most stable structures of adsorption of CO and HCO_2 on a Pt surface are known, with CO adsorbing in a top configuration[61,66] and HCO_2 in a bidentate configuration with both O atoms interacting symmetrically with Pt.[13] The CO and HCO_2 adsorption structures optimized on a negatively charged Pt surface in water are shown in Figure 6, while adsorption energies for CO, HCO_2, and CO_2H are shown in Table 7 for water and Table 8 for acetonitrile.

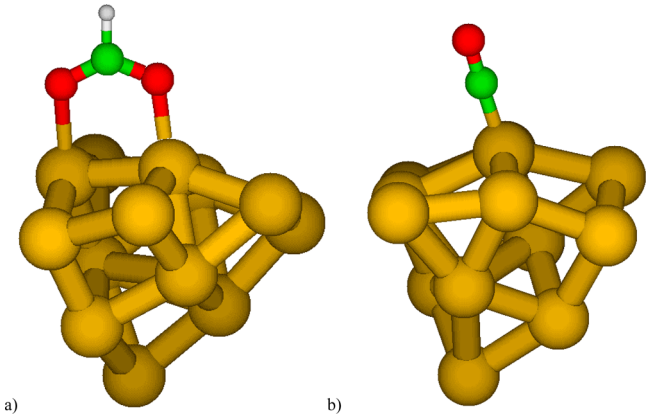

Figure 6. Minimum energy structures of HCO_2 and CO adsorbed over the negatively charged Pt13 cluster calculated at the B3LYP/SDD-6-311+G(d,p) level in a water solvent.

The most interesting aspect of the data reported in Tables 7 and 8 is that the interaction energy of HCO_2 is smaller than that of CO_2H. As both energies are referred, in order to ease the comparison, to the same reactants (the cluster and $CO_2H\cdot$), this means that CO_2H_{ads} is significantly more stable (about 15 kcal/mol) than the adsorbed formate. To the best of our knowledge, this is an aspect that is presently not taken in consideration in the analysis of the reaction kinetics of CO_2 on Pt electrodes; in view of the results here reported, this aspect should deserve more attention. Because the structure of the two isomers differs substantially, it is not clear whether the energetic barrier by which they are separated may readily be overcome during the electrochemical reaction. Also, the calculated adsorption energy for CO is high, as expected. This is consistent with the fact that CO is a known poisoning agent for Pt electrodes. The calculated vibrational frequencies for the stretching of adsorbed CO are 1851 and 1948 cm^{-1} in water and 1904 and 1989 cm^{-1} in acetonitrile on neutral and negatively charged Pt13 clusters, respectively. The vibrational

Table 7. Adsorption Free Energies (Absolute Values) Computed at the B3LYP/SDD-6-311+G(d,p) Level in Water for CO_2H, HCO_2, and CO on Pt13 and Pt20 Clusters Using Eq 1[a]

cluster	charge	multiplicity	ΔG (kcal/mol) LANL2DZ D95	ΔG (kcal/mol) SDD 6-311+G(d,p)	ΔG (kcal/mol) CRENBL 6-311+G(d,p)
			CO_2H		
Pt13	0	2	66.6	60.0	62.5
Pt13	−1	1	70.3	63.0	65.4
Pt20	0	14	66.1	57.7	59.8
			HCO_2		
Pt13	0	2	58.0	45.2	46.9
Pt13	−1	1	62.4	50.0	52.6
Pt20	0	14	53.1	40.8	42.4
			CO		
Pt13	0	3	37.2	30.3	33.0
Pt13	−1	2	44.5	36.1	36.6
Pt20	0	15	34.0	29.0	30.1

[a]The HCO_2 adsorption energies are calculated relatively to decomposition to the Pt cluster and CO_2H·. The entropic correction, not included in the reported free energies, is about +13 kcal/mol for CO_2H and HCO_2 adsorption and about +10 kcal/mol for CO adsorption (at the B3LYP/SDD-6-311+G(d,p) level on Pt13).

Table 8. Adsorption Free Energies (Absolute Values) Computed at the B3LYP/SDD-6-311+G(d,p) Level in Acetonitrile for CO_2H, HCO_2, and CO on Pt13 and Pt20 Clusters Using Eq 1[a]

cluster	charge	multiplicity	ΔG (kcal/mol) LANL2DZ D95	ΔG (kcal/mol) SDD 6-311+G(d,p)	ΔG (kcal/mol) CRENBL 6-311+G(d,p)
			CO_2H		
Pt13	0	2	63.5	59.5	61.2
Pt13	−1	1	67.7	62.4	64.3
Pt20	0	14	63.8	57.9	59.4
			HCO_2		
Pt13	0	2	60.6[b]	45.8	48.5
Pt13	−1	1	55.9[b]	50.8	53.2
Pt20	0	14	53.7	39.5	42.2
			CO		
Pt13	0	3	37.2	30.3	31.1
Pt13	−1	2	42.2	36.3	36.7
Pt20	0	15	37.1	28.9	30.6

[a]The HCO_2 adsorption energies are calculated relatively to decomposition to the Pt cluster and CO_2H·. The entropic correction, not included in the reported free energies, is about +13 kcal/mol for CO_2H and HCO_2 adsorption and about +10 kcal/mol for CO adsorption (at the B3LYP/SDD-6-311+G(d,p) level on Pt13). [b]These data are not in line with the expected trend. The adsorption free energies were thus recalculated using the LANLTZ-6-311+G(d,p) basis set, obtaining adsorption energies of 48.8 and 54.5 kcal/mol for the uncharged and the negatively charged clusters, respectively.

frequency of adsorbed CO in acetonitrile on the negatively charged cluster is in reasonable agreement with the FTIR measurement of Tomita et al.,[65] who attributed to the formation of CO the peak of 2079 cm^{-1} measured on Pt electrodes exposed to CO_2 in acetonitrile in the presence of a water concentration of 10.5 mM.

4. CONCLUSIONS

In the present work a theoretical analysis of some thermodynamic and kinetic aspects of CO_2 electrochemical reactivity at the Pt electrode has been performed modeling the Pt surface through charged clusters and performing DFT calculations using an implicit solvent model. The main results can be summarized as follows.

(1) CO_2 adsorption is highly favored on negatively charged clusters and takes place passing from a well-defined transition state. A reasonable interpretation of these computational results is that an electron-transfer reaction will take place contextually to CO_2 adsorption, probably in proximity of the transition state. Our proposal is that the charge transfer will take place mostly on the Pt surface and will be followed by the establishment of a dative bond between a Pt surface atom and CO_2, which will result in a significant charge transfer to CO_2. The computational evidence suggests that the electrodic CO_2 adsorption reaction may be described as

$$CO_2 + Pt\_surf + e^- \rightarrow CO_{2ads}{}^-$$

(2) The present results suggest that the formation of the $CO_2^{\bullet -}$ aqueous species is significantly unfavored from an energetic standpoint with respect to $CO_{2ads}{}^-$ and that its main fate, if formed, would be most likely that of getting adsorbed again on the Pt surface.

(3) The calculation of the pK_a of $CO_{2ads}{}^-$ showed that its protonation reaction is thermodynamically favored in most electrochemical conditions used for CO_2 reduction.

(4) An important finding of this work is that the free-energy difference between adsorbed formate and adsorbed CO_2H favors the latter. It is our opinion that the interconversion kinetics of these two species at a Pt surface should be the object of future research.

Combining the results of the present study with experimental evidence of the identities of the major products of the reduction of CO_2 and Pt electrodes in water and acetonitrile as a function of the operative conditions, in particular referring to the works of Tomita et al.[65] and of Hori et al.,[2] we formulate and propose a tentative global mechanism for CO_2 reduction at Pt electrodes (Figure 7).

The proposed reaction mechanism is in many ways self-explanatory. It involves the formation of the reaction intermediates that have been presented in this work, with the addition of adsorbed formic acid (HCO_2H_{ads}), and it comprises two electron-transfer reactions and two protonation reactions, as all the proposed mechanisms for CO_2 reduction do. The possible reaction products are formic acid (HCO_2H^{sol}), oxalate in its various ionic states ($[CO_2{}^-]_2{}^{sol}$, $HCO_2CO_2{}^{-sol}$), the formate anion ($HCO_2{}^{-sol}$), and CO. Several routes are possible for the formation of the reaction products. A pathway by which formate is formed from the reaction between two CO_2H_{ads} surface species is introduced in the mechanism to account for the evidence that at high CO_2 partial pressure the main product of CO_2 reduction shifts from H_2 to formic acid,[9] suggesting that a dual site surface mechanism is active. On the whole, this mechanism is consistent with many proposals already reported in the literature.[1] It is, for example, consistent with the proposal of Cuesta et al. that formate[12] may be a key intermediate in the oxidation of formic acid and with the reaction paths A, B, G, and H as summarized by Chaplin and Wragg,[1] from which it differs, however, for the formate and oxalate mechanisms. The main feature of the proposed mechanism is the identification of

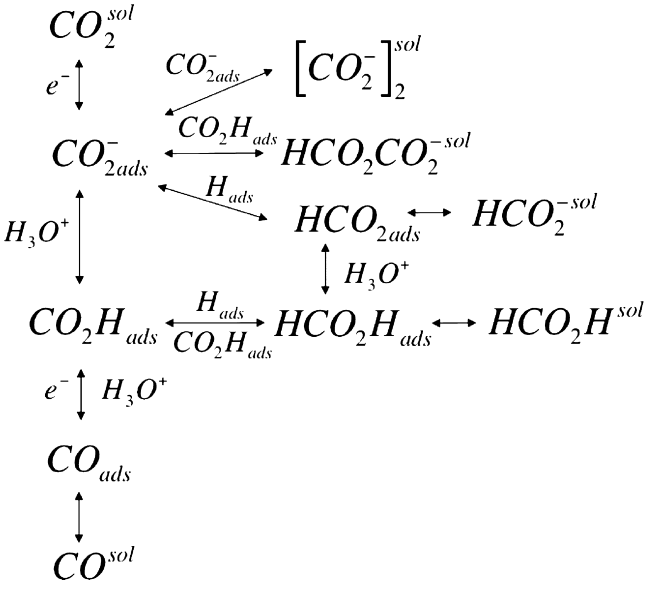

Figure 7. Proposed mechanism for the cathodic set of reactions that may be active during the reduction of CO_2 at Pt electrodes in acetonitrile and water.

four main surface intermediates: CO_{2ads}^-, CO_2H_{ads}, HCO_{2ads}, and HCO_2H_{ads}.

■ ASSOCIATED CONTENT

● Supporting Information

Structures and vibrational frequencies (only for Pt13 clusters) in water and acetonitrile solvent for different spin multiplicities and total charges of Pt13 and Pt20 clusters, CO_2 adsorbed on Pt clusters, transition states for CO_2 adsorption on Pt13 clusters, CO_2 (2 H_2O) adsorbed on Pt13 clusters, COOH adsorbed on Pt clusters, HCO_2 adsorbed on Pt clusters, and CO adsorbed on Pt clusters. This material is available free of charge via Internet.

■ AUTHOR INFORMATION

Corresponding Author

*Tel: +39-02-23993176. Fax +39-02-23993180. E-mail: carlo.cavallotti@polimi.it.

Notes

The authors declare no competing financial interest.

■ ACKNOWLEDGMENTS

The authors are grateful to Politecnico di Milano for the financial support received from the FARB 2011 initiative.

■ REFERENCES

(1) Chaplin, R. P. S.; Wragg, A. A. Effects of process conditions and electrode material on reaction pathways for carbon dioxide electroreduction with particular reference to formate formation. *J. Appl. Electrochem.* **2003**, *33*, 1107−1123.

(2) Hori, Y. Electrochemical CO_2 Reduction on Metal Electrodes. In *Modern Aspects of Electrochemistry, No 42*; Vayenas, C. G., White, R. E., GamboaAldeco, M. E., Eds.; Springer: New York, 2008; pp 89−189.

(3) Kaneco, S.; Iiba, K.; Ohta, K.; Mizuno, T. Reduction of carbon dioxide to petrochemical intermediates. *Energy Sources* **2000**, *22*, 127−135.

(4) Lukaszewski, M.; Siwek, H.; Czerwinski, A. Electrosorption of carbon dioxide on platinum group metals and alloys—A review. *J. Solid State Electrochem.* **2009**, *13*, 813−827.

(5) Freund, H. J.; Roberts, M. W. Surface chemistry of carbon dioxide. *Surf. Sci. Rep.* **1996**, *25*, 225−273.

(6) Jitaru, M.; Lowy, D. A.; Toma, M.; Toma, B. C.; Oniciu, L. Electrochemical reduction of carbon dioxide on flat metallic cathodes. *J. Appl. Electrochem.* **1997**, *27*, 875−889.

(7) Sanchez-Sanchez, C. M.; Montiel, V.; Tryk, D. A.; Aldaz, A.; Fujishima, A. Electrochemical approaches to alleviation of the problem of carbon dioxide accumulation. *Pure Appl. Chem.* **2001**, *73*, 1917−1927.

(8) Lamy, E.; Nadjo, L.; Saveant, J.-M. Standard potential and kinetic parameters of the electrochemical reduction of carbon dioxide in dimethylformamide. *J. Electroanal. Chem.* **1977**, *78*, 403.

(9) Hara, K.; Kudo, A.; Sakata, T. Electrochemical reduction of carbon dioxide under high pressure on various electrodes in an aqueous electrolyte. *J. Electroanal. Chem.* **1995**, *391*, 141−147.

(10) Aylmer-Kelly, A. W. B.; Bewick, A.; Cantrill, P. R.; Tuxford, A. M. Studies of electrochemically generated reaction intermediates using modulated specular reflectance spectroscopy. *Faraday Discuss.* **1973**, *56*, 96−107.

(11) Chandrasekaran, K.; Bockris, J. O. In-situ spectroscopic investigation of adsorbed intermediate radicals in electrochemical reactions: CO_2^- on platinum. *Surf. Sci.* **1987**, *185*, 495−514.

(12) Cuesta, A.; Cabello, G.; Gutierrez, C.; Osawa, M. Adsorbed formate: The key intermediate in the oxidation of formic acid on platinum electrodes. *Phys. Chem. Chem. Phys.* **2011**, *13*, 20091−20095.

(13) Osawa, M.; Komatsu, K.-i.; Samjeske, G.; Uchida, T.; Ikeshoji, T.; Cuesta, A.; Gutierrez, C. The Role of Bridge-Bonded Adsorbed Formate in the Electrocatalytic Oxidation of Formic Acid on Platinum. *Angew. Chem., Int. Ed.* **2011**, *50*, 1159−1163.

(14) Wang, H.-F.; Liu, Z.-P. Formic Acid Oxidation at Pt/H_2O Interface from Periodic DFT Calculations Integrated with a Continuum Solvation Model. *J. Phys. Chem. C* **2009**, *113*, 17502− 17508.

(15) Ishikawa, Y.; Mateo, J. J.; Tryk, D. A.; Cabrera, C. R. Direct molecular dynamics and density-functional theoretical study of the electrochemical hydrogen oxidation reaction and underpotential deposition of H on Pt(111). *J. Electroanal. Chem.* **2007**, *607*, 37−46.

(16) Shi, C.; O'Grady, C. P.; Peterson, A. A.; Hansen, H. A.; Norskov, J. K. Modeling CO_2 reduction on Pt(111). *Phys. Chem. Chem. Phys.* **2013**, *15*, 7114−7122.

(17) Becke, A. D. Density functional thermochemistry. III. The role of exact exchange. *J. Chem. Phys.* **1993**, *98*, 5648−5652.

(18) Lee, C.; Yang, W.; Parr, R. G. Development of the Colle-Salvetti correlation-energy formula into a functional of the electron density. *Phys. Rev. B: Condens. Matter Mater. Phys.* **1988**, *37*, 785−789.

(19) Tirado-Rives, J.; Jorgensen, W. L. Performance of B3LYP density functional methods for a large set of organic molecules. *J. Chem. Theory Comput.* **2008**, *4*, 297−306.

(20) Cavallotti, C.; Rota, R.; Carra, S. Quantum chemistry computation of rate constants for reactions involved in the first aromatic ring formation. *J. Phys. Chem. A* **2002**, *106*, 7769−7778.

(21) Moiani, D.; Cavallotti, C.; Famulari, A.; Schmuck, C. Oxoanion binding by guanidiniocarbonylpyrrole cations in water: A combined DFT and MD investigation. *Chem.—Eur. J.* **2008**, *14*, 5207−5219.

(22) Gao, H.; Wei, X.; Liu, X.; Yan, T. Comparison of Different Theory Models and Basis Sets in the Calculations of Structures and ^{13}C NMR Spectra of [Pt(en)(CBDCA−O, O′)], an Analogue of the Antitumor Drug Carboplatin. *J. Phys. Chem. B* **2010**, *114*, 4056−4062.

(23) Wysokinski, R.; Michalska, D. The performance of different density functional methods in the calculation of molecular structures and vibrational spectra of platinum(II) antitumor drugs: Cisplatin and carboplatin. *J. Comput. Chem.* **2001**, *22*, 901−912.

(24) Zhao, Y.; Truhlar, D. G. The M06 suite of density functionals for main group thermochemistry, thermochemical kinetics, non-covalent interactions, excited states, and transition elements: Two new functionals and systematic testing of four M06-class functionals and 12 other functionals. *Theor. Chem. Acc.* **2008**, *120*, 215−241.

(25) Hay, P. J.; Wadt, W. R. Ab initio effective core potentials for molecular calculations. Potentials for the transition metal atoms Sc to Hg. *J. Chem. Phys.* **1985**, *82*, 270−283.
(26) Hay, P. J.; Wadt, W. R. Ab initio effective core potentials for molecular calculations. Potentials for K to Au including the outermost core orbitals. *J. Chem. Phys.* **1985**, *82*, 299−310.
(27) Wadt, W. R.; Hay, P. J. Ab initio effective core potentials for molecular calculations. Potentials for main group elements Na to Bi. *J. Chem. Phys.* **1985**, *82*, 284−298.
(28) Dunning, T. H. J.; Hay, P. J. In *Modern Theoretical Chemistry*; Schaefer, H. F., III, Ed.; Plenum: New York, 1976; pp 1−28.
(29) Bergner, A.; Dolg, M.; Kuchle, W.; Stoll, H.; Preuss, H. Ab-initio energy-adjusted pseudopotentials for elements of groups 13−17. *Mol. Phys.* **1993**, *80*, 1431−1441.
(30) Kaupp, M.; Schleyer, P. V.; Stoll, H.; Preuss, H. Pseudopotential approaches to Ca, Sr, and Ba hydrides. Why are some alkaline earth MX_2 compounds bent? *J. Chem. Phys.* **1991**, *94*, 1360−1366.
(31) Ross, R. B.; Powers, J. M.; Atashroo, T.; Ermler, W. C.; Lajohn, L. A.; Christiansen, P. A. Ab Initio relativistic effective potentials with spin-orbit operators. IV. Cs through Rn. *J. Chem. Phys.* **1990**, *93*, 6654−6670.
(32) Shimanouchi, T. *Tables of Molecular Vibrational Frequencies Consolidated Vol. I*; National Bureau of Standards, 1972.
(33) Chung, S. C.; Kruger, S.; Pacchioni, G.; Rosch, N. Relativistic effects in the electronic structure of the monoxides and monocarbonyls of Ni, Pd and Pt: Local and gradient-corrected density functional calculations. *J. Chem. Phys.* **1995**, *102*, 3695−3702.
(34) Pacchioni, G.; Chung, S. C.; Kruger, S.; Rosch, N. Is CO chemisorbed on Pt anomalous compared with Ni and Pd? An example of surface chemistry dominated by relativistic effects. *Surf. Sci.* **1997**, *392*, 173−184.
(35) Sicolo, S.; Pacchioni, G. A DFT study of PtAu bimetallic clusters adsorbed on MgO/Ag(100) ultrathin films. *Phys. Chem. Chem. Phys.* **2010**, *12*, 6352−6356.
(36) Daramola, D. A.; Botte, G. G. Theoretical study of ammonia oxidation on platinum clusters − Adsorption of ammonia and water fragments. *Comput. Theor. Chem.* **2012**, *989*, 7−17.
(37) Chou, J. P.; Hsing, C. R.; Wei, C. M.; Cheng, C.; Chang, C. M. Ab initio random structure search for 13-atom clusters of fcc elements *J. Phys.: Condens. Matter* **2013**, *25*.
(38) Cances, E.; Mennucci, B.; Tomasi, J. A new integral equation formalism for the polarizable continuum model: Theoretical background and applications to isotropic and anisotropic dielectrics. *J. Chem. Phys.* **1997**, *107*, 3032−3041.
(39) Mennucci, B.; Cances, E.; Tomasi, J. Evaluation of solvent effects in isotropic and anisotropic dielectrics and in ionic solutions with a unified integral equation method: Theoretical bases, computational implementation, and numerical applications. *J. Phys. Chem. B* **1997**, *101*, 10506−10517.
(40) Motaghiani, S.; Mirabbaszadeh, K. Density functional study of platinum polyyne monomer, oligomer, and polymer: Ground state geometrical and electronic structures. *Int. J. Quantum Chem.* **2013**, *113*, 1650−1659.
(41) Cramer, C. J.; Truhlar, D. G. Density functional theory for transition metals and transition metal chemistry. *Phys. Chem. Chem. Phys.* **2009**, *11*, 10757−10816.
(42) Cappelli, C.; Monti, S.; Scalmani, G.; Barone, V. On the Calculation of Vibrational Frequencies for Molecules in Solution Beyond the Harmonic Approximation. *J. Chem. Theory Comput.* **2010**, *6*, 1660−1669.
(43) Marenich, A. V.; Cramer, C. J.; Truhlar, D. G. Universal Solvation Model Based on Solute Electron Density and on a Continuum Model of the Solvent Defined by the Bulk Dielectric Constant and Atomic Surface Tensions. *J. Phys. Chem. B* **2009**, *113*, 6378−6396.
(44) Bryantsev, V. S.; Diallo, M. S.; Goddard, W. A., III. Calculation of solvation free energies of charged solutes using mixed cluster/continuum models. *J. Phys. Chem. B* **2008**, *112*, 9709−9719.
(45) Ho, J.; Coote, M. L. First-principles prediction of acidities in the gas and solution phase. *Wiley Interdiscip. Rev.: Comput. Mol. Sci.* **2011**, *1*, 649−660.
(46) Ho, J.; Coote, M. L. pK_a Calculation of Some Biologically Important Carbon Acids - An Assessment of Contemporary Theoretical Procedures. *J. Chem. Theory Comput.* **2009**, *5*, 295−306.
(47) Reed, A. E.; Curtiss, L. A.; Weinhold, F. Intermolecular interactions from a natural bond orbital, donor−acceptor viewpoint. *Chem. Rev. (Washington, DC, U.S.)* **1988**, *88*, 899−926.
(48) Besler, B. H.; Merz, K. M.; Kollman, P. A. Atomic charges derived from semiempirical methods. *J. Comput. Chem.* **1990**, *11*, 431−439.
(49) Batsanov, S. S. Van der Waals radii of elements. *Inorg. Mater.* **2001**, *37*, 871−885.
(50) Frisch, M. J.; Trucks, G. W.; Schlegel, H. B.; Scuseria, G. E.; Robb, M. A.; Cheeseman, J. R.; Scalmani, G.; Barone, V.; Mennucci, B.; Petersson, G. A.; Nakatsuji, H.; Caricato, M.; Li, X.; Hratchian, H. P.; Izmaylov, A. F.; Bloino, J.; Zheng, G.; Sonnenberg, J. L.; Hada, M.; Ehara, M.; Toyota, K.; Fukuda, R.; Hasegawa, J.; Ishida, M.; Nakajima, T.; Honda, Y.; Kitao, O.; Nakai, H.; Vreven, T.; Montgomery, J. A., Jr.; Peralta, J. E.; Ogliaro, F.; Bearpark, M.; Heyd, J. J.; Brothers, E.; Kudin, K. N.; Staroverov, V. N.; Kobayashi, R.; Normand, J.; Raghavachari, K.; Rendell, A.; Burant, J. C.; Iyengar, S. S.; Tomasi, J.; Cossi, M.; Rega, N.; Millam, N. J.; Klene, M.; Knox, J. E.; Cross, J. B.; Bakken, V.; Adamo, C.; Jaramillo, J.; Gomperts, R.; Stratmann, R. E.; Yazyev, O.; Austin, A. J.; Cammi, R.; Pomelli, C.; Ochterski, J. W.; Martin, R. L.; Morokuma, K.; Zakrzewski, V. G.; Voth, G. A.; Salvador, P.; Dannenberg, J. J.; Dapprich, S.; Daniels, A. D.; Farkas, Ö.; Foresman, J. B.; Ortiz, J. V.; Cioslowski, J.; Fox, D. J. *Gaussian 09*, revision A.1; Gaussian, Inc.: Wallingford CT, 2009.
(51) Schaftenaar, G.; Noordik, J. H. Molden: A pre- and post-processing program for molecular and electronic structures. *J. Comput.-Aided Mol. Des.* **2000**, *14*, 123−134.
(52) Weigend, F.; Ahlrichs, R. Balanced basis sets of split valence, triple zeta valence and quadruple zeta valence quality for H to Rn: Design and assessment of accuracy. *Phys. Chem. Chem. Phys.* **2005**, *7*, 3297−3305.
(53) Weigend, F.; Baldes, A. Segmented contracted basis sets for one- and two-component Dirac-Fock effective core potentials *J. Chem. Phys.* **2010**, *133*.
(54) Roy, L. E.; Hay, P. J.; Martin, R. L. Revised basis sets for the LANL effective core potentials. *J. Chem. Theory Comput.* **2008**, *4*, 1029−1031.
(55) Woon, D. E.; Dunning, T. H. Gaussian basis sets for use in correlated molecular calculations. 5. Core-valence basis sets for boron through neon. *J. Chem. Phys.* **1995**, *103*, 4572−4585.
(56) Feller, D. The role of databases in support of computational chemistry calculations. *J. Comput. Chem.* **1996**, *17*, 1571−1586.
(57) Schuchardt, K. L.; Didier, B. T.; Elsethagen, T.; Sun, L.; Gurumoorthi, V.; Chase, J.; Li, J.; Windus, T. L. Basis set exchange: A community database for computational sciences. *J. Chem. Inf. Model.* **2007**, *47*, 1045−1052.
(58) Airola, M. B.; Morse, M. D. Rotationally resolved spectroscopy of Pt-2. *J. Chem. Phys.* **2002**, *116*, 1313−1317.
(59) Abild-Pedersen, F.; Andersson, M. P. CO adsorption energies on metals with correction for high coordination adsorption sites − A density functional study. *Surf. Sci.* **2007**, *601*, 1747−1753.
(60) Yoshinobu, J.; Kawai, M. Initial adsorption sites of CO on Pt(111) and Ni(100) at low temperature. *Surf. Sci.* **1996**, *363*, 105−111.
(61) Gruene, P.; Fielicke, A.; Meijer, G.; Rayner, D. M. The adsorption of CO on group 10 (Ni, Pd, Pt) transition-metal clusters. *Phys. Chem. Chem. Phys.* **2008**, *10*, 6144−6149.
(62) Schimka, L.; Harl, J.; Stroppa, A.; Grueneis, A.; Marsman, M.; Mittendorfer, F.; Kresse, G. Accurate surface and adsorption energies from many-body perturbation theory. *Nat. Mater.* **2010**, *9*, 741−744.
(63) Wang, Y.; de Gironcoli, S.; Hush, N. S.; Reimers, J. R. Successful a priori modeling of CO adsorption on pt(111) using periodic hybrid density functional theory. *J. Am. Chem. Soc.* **2007**, *129*, 10402−10407.

(64) Yudanov, I. V.; Genest, A.; Schauermann, S.; Freund, H.-J.; Roesch, N. Size Dependence of the Adsorption Energy of CO on Metal Nanoparticles: A DFT Search for the Minimum Value. *Nano Lett.* **2012**, *12*, 2134−2139.
(65) Tomita, Y.; Teruya, S.; Koga, O.; Hori, Y. Electrochemical reduction of carbon dioxide at a platinum electrode in acetonitrile-water mixtures. *J. Electrochem. Soc.* **2000**, *147*, 4164−4167.
(66) Ge, Q.; Song, C.; Wang, L. A density functional theory study of CO adsorption on Pt-Au nanoparticles. *Comput. Mater. Sci.* **2006**, *35*, 247−253.